



ELSEVIER

Physica B 315 (2002) 64–73

PHYSICA B

www.elsevier.com/locate/physb

Electronic and structural properties of LaSb and LaBi

G. Vaitheeswaran, V. Kanchana, M. Rajagopalan*

Department of Physics, Anna University, Chennai 600 025, India

Received 1 August 2001; received in revised form 3 October 2001

Abstract

The electronic structure and structural properties of LaSb and LaBi are studied by means of the self-consistent tight binding linear muffin tin orbital method. The relative stabilities of LaSb and LaBi at high pressures in the Rock salt, Primitive tetragonal and CsCl structures are analysed. At compressed volumes, these compounds are found to favour the tetragonal phase rather the CsCl phase, which can be seen from the total energy curves. The transition from B1 to PT occurs around 8.6 and 11.2 GPa in LaSb and LaBi, respectively. The ground state properties of these compounds such as equilibrium lattice constant, bulk modulus are calculated and are in good agreement with the experimental results. The band structure and density of states are plotted for B1 and tetragonal phase and are compared with the available literature. © 2002 Elsevier Science B.V. All rights reserved.

PACS: 63.20.k; 74.62

Keywords: Band structure; High pressure

1. Introduction

The rare-earth monpnictides with the NaCl structure have recently attracted particular interest because of various anomalous physical properties [1]. As a proper reference material having no occupied 4f states, the lanthanum pnictides, LaX has been investigated both experimentally and theoretically.

The de Haas–van Alphen effect (dHvA) has been studied for LaSb by Kitazawa et al. [2]. Hasegawa has calculated the Fermi surface using the relativistic APW method [3]. The electronic structure of LaSb, in particular its Fermi surface

topology has been intensively studied theoretically [3,4] and experimentally [5,6] because LaSb has no 4f electrons and is regarded as a good non-magnetic reference to CeSb and USb, which exhibit anomalous physical properties [7–9].

In addition photoemission spectroscopy studies has been performed by Kumigashira et al. [10] to obtain the electronic band structure of LaSb. Acoustic de Haas–van Alphen effect in LaSb and CeSb has been reported by Settai et al. [11]. Similarly, optical reflectivity spectra were measured for CeSb and LaSb by Kwon et al. [12]. The transport property (resistivity measurements) of LaSb, YbAs and YbP has been studied by Kasuya et al. [13].

Hasegawa [3] has calculated the electronic band structure of LaSb and LaBi. Recently Hayashi et al. [14] using synchrotron radiation reported

*Corresponding author. Tel.: +91-14-2213023; fax: +91-44-2352870.

E-mail address: mraja@eth.net (M. Rajagopalan).

that LaSb undergoes a crystallographic transition from B1 (NaCl) to Tetragonal phase around 11 GPa with $c/a = 0.82$. The volume collapse is reported to be 10.1%. Similarly Leger et al. [15] has reported a comparative volume behaviour of CeSb and LaSb up to 25 GPa and from the compression curves, the volume reduction for both CeSb and LaSb are found to be equal in the pressure range investigated. It is also found that CeSb and LaSb have same Bulk moduli. As far as LaBi is concerned, the bulk modulus data in the B1 phase is reported by Benedict [16]. So far, there is no theoretical study on the high-pressure structural phase transformation of LaSb and LaBi. Hence, an attempt has been made in the present work to compute the electronic structure, ground state properties and high-pressure structural phase transformations of these two compounds using the self-consistent tight binding linear muffin tin orbital method (TB-LMTO). In the present work, the band structure, density of states and bulk modulus are computed and compared with the available theoretical and experimental results. The values obtained in the present study are in good agreement with those of others [3,14–18]. The rest of the paper is organized as follows. In Section 2, the crystallographic data and computational details of these Lanthanum pnictides are given. The results are discussed in Section 3. The conclusions are given in the last section.

2. Structural aspects and computational details

The Lanthanum monopnictides crystallize in the simple rock salt structure (B1 type) with the space group symmetry $Fm\bar{3}m$ where the La atom is positioned at (0,0,0) and the pnictogen at $(\frac{1}{2}, \frac{1}{2}, \frac{1}{2})$. The structure of the high-pressure phase of LaSb is tetragonal which can be viewed as a distorted CsCl structure (B2 type) [14,15] with La at (0,0,0) and Pnictogen at $(\frac{1}{2}, \frac{1}{2}, \frac{1}{2})$ and the space group symmetry is $P4/mmm$.

The band structure for both B1 and the high-pressure phase, and the total energies within the atomic-sphere approximation were obtained by means of the TB-LMTO method [19,20]. von-Barth and Hedin parameterization scheme has

been used for the exchange correlation potential [21] within the local density approximation (LDA). The accuracy of total energies obtained with in the density-functional theory, often even using the LDA, is in many cases sufficient to predict which structure at a given pressure has the lowest free energy [22]. In the atomic sphere approximation [23], crystal is divided into space filling spheres centered on each of the atomic site. Combined corrections are also included, which account for the non-spherical shape of the atomic spheres and the truncation of the higher partial waves inside the spheres to minimize the errors in the LMTO method. The Wigner-Seitz sphere radius is chosen in such a way that the sphere boundary potential is minimum and the charge flow between the two atoms is in accordance with the electro negativity criteria. s, p, d and f partial waves are included. The tetrahedron method [24] of the Brillouin zone (K space) integration has been used with 1543K points in the irreducible part of the Brillouin zone for B1, and 4630K points in PT and 443K points in B2 phases. E and K convergence is also checked. The following basis orbitals are used in LaSb and LaBi:

La: $6s^2, 5p^6, 5d^1, 4f^0$
 Sb: $5s^2, 5p^3, 5d^0$
 Bi: $6s^2, 6p^3, 6d^0$

It is well known that the LMTO method gives accurate results for densely packed structures and since the NaCl structure is a loosely packed structure, it becomes necessary to include empty spheres [25,26,30]. Two empty spheres are included in this structure without breaking the crystal symmetry at (0.25, 0.25, 0.25) and (0.75, 0.75, 0.75).

3. Results and discussions

3.1. Total energy calculation and high-pressure structural phase transformations

In order to study the structural phase stability for each of these compounds the total energies are calculated in a manner similar to our earlier works

[27,28] for B1, PT and B2 structures by reducing the volume from $1.05V_0$ to $0.6V_0$ where ' V_0 ' is the experimental equilibrium volume. The variations of the total energies with relative volume for all these compounds are given in Fig. 1. From the graphs, it is evident that B1 phase is a stable phase at ambient pressure. PT is positioned above B1 and B2 phase lies above the primitive tetragonal phase. Experimental work of Hayashi et al. [14] reports a crystallographic transition in LaSb from B1 to Primitive tetragonal phase, around 11 GPa. PT can be viewed as a distorted CsCl structure and so calculations were performed for both Primitive tetragonal and CsCl structures to determine which of these two is favoured more under pressure. The c/a ratio in the tetragonal phase is obtained by total energy minimization and it is found to be 0.82, 0.84 in the case of LaSb and LaBi, which is in good agreement with the experimental value [14].

The calculated total energies are fitted to the Birch Equation of state [29] to obtain the pressure volume relation. The graphs connecting the pressure and relative volume in B1 and PT phases are shown in Fig. 2. The pressure is obtained by taking the volume derivative of the total energy.

The Bulk Modulus

$$B = -V_0 dP/dV \quad (1)$$

is also calculated from the P - V relation.

The theoretically calculated equilibrium lattice constant and the Bulk modulus for B1 and PT structures are given in Table 1 and 2 and are compared with the available experimental and theoretical works. The structural phase stability is determined by calculating Gibb's free energy (G) [36] for B1 and PT that is

$$G = E_{\text{tot}} + PV - TS. \quad (2)$$

Since the theoretical calculations are performed at 0 K Gibb's free energy becomes equal to the enthalpy (H)

$$H = E_{\text{tot}} + PV. \quad (3)$$

At a given pressure a stable structure is one for which enthalpy has its lowest value and the transition pressures are calculated at which the enthalpies for the two phases are equal. The transition pressure from B1 to PT structure, volume reductions are given in Table 3 and are compared with the earlier literature [14].

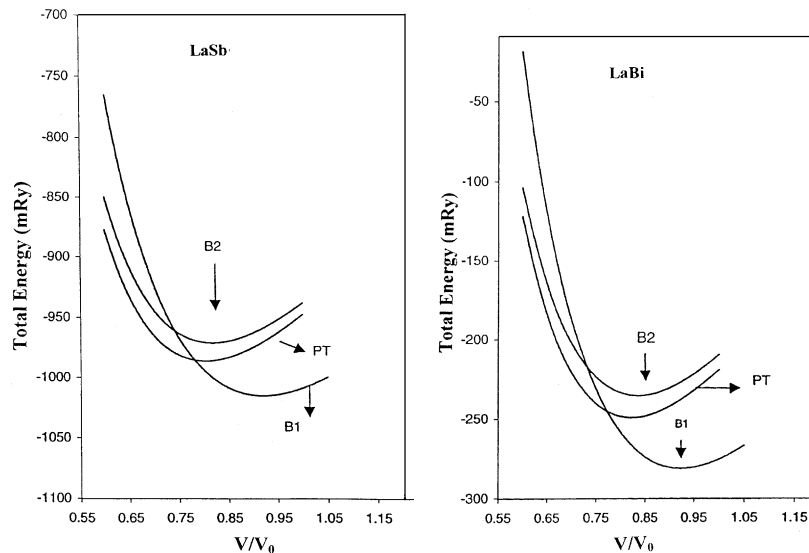


Fig. 1. (a) Calculated total energy ($-29929.00 +$) Ry vs. relative volume for LaSb. (b) Calculated total energy ($-60017.00 +$) Ry vs. relative volume for LaBi.

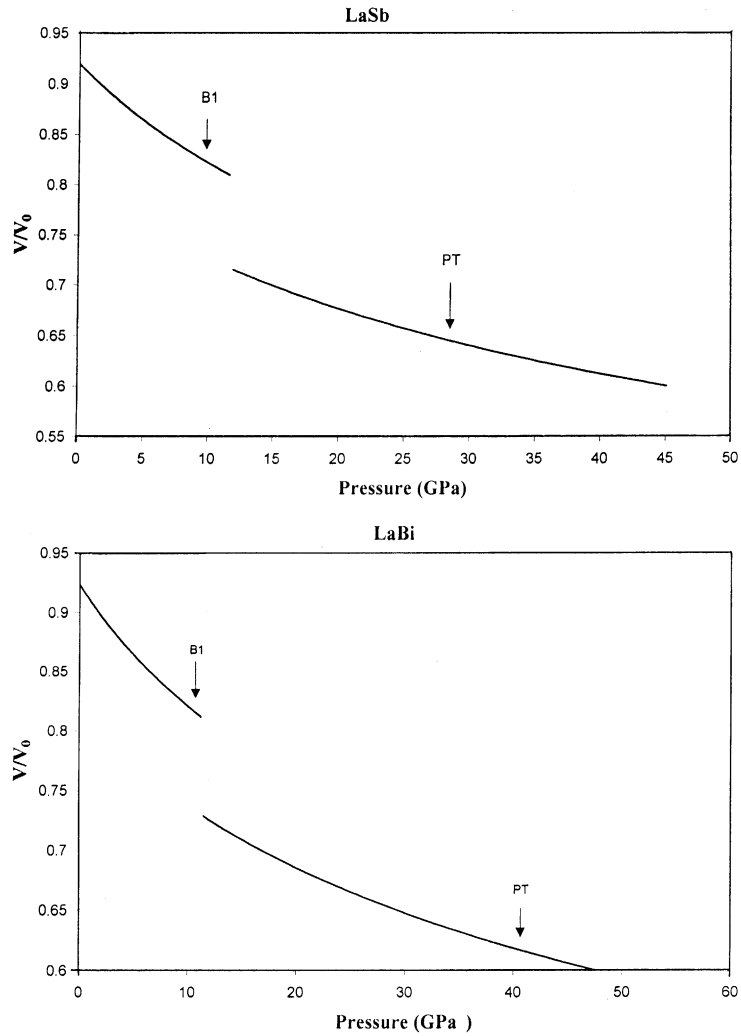


Fig. 2. Calculated pressure volume relation in the B1 and PT structures for (a) LaSb and (b) LaBi.

Table 1
Structural and cohesive properties of LaSb

LaSb	B1		PT	
	Present	Expt.	Present	Expt.
Lattice parameter (\AA)	$a = 6.297$	6.475	$a = 3.931$ $c = 3.224$ $c/a = 0.82$	4.019 3.279 0.82
$N(E_F)$ (states/Ry/cell)	4.2	—	14.25	—
Bulk modulus (GPa)	69.76	—	116.24	—
γ (mJ/mol K^2)	0.72	0.80	—	—

Table 2
Structural and cohesive properties of LaBi

LaBi	B1		PT	
	Present	Expt.	Present	Expt.
Lattice parameter (Å)	$a = 6.392$	6.564	$a = 3.946$ $c = 3.314$ $c/a = 0.83$	—
$N(E_F)$ (states/Ry/cell)	4.58	—	14.73	—
Bulk modulus (GPa)	65.18	55 ^a	121.33	—
γ (mJ/mol K ²)	0.79	1.71	—	—

^a Ref. [18].

Table 3
Calculated transition pressure and volume collapse

Compound	Transition pressure (GPa)		Volume collapse (%)	
	Present	Expt.	Present	Expt.
LaSb	8.6	11	10.7	10.1
LaBi	11.2	—	8.9	—

From the graph connecting the total energy and relative volume one can clearly see the relative stabilities of the high-pressure phases of LaSb and LaBi. As the Primitive tetragonal phase can be viewed as a distorted CsCl structure, one may think of a transition from B1 to PT as well as from B1 to B2. Hence, total energies were computed for B1, PT and B2 structures. In both the compounds, B1 phase is stable at ambient conditions. Between the two high-pressure phases B2 and PT, it is found that the tetragonal phase is energetically lower than B2. The basic requirement for a phase to be stable is that the Gibb's free energy should be minimum. The B2 phase lies above the tetragonal phase in both LaSb and LaBi and the energy difference between the two phases is around 15 mRy in the case of LaSb and 14 mRy in LaBi. Hence, the B2 phase does not compete, as a high-pressure phase in these ranges of volumes and a transition from B1 to PT is only possible in both the compounds.

The structural transformation of LaSb is similar to that of CeSb in which the high-pressure phase is of primitive tetragonal structure. The transition from B1 to PT in LaSb occurs around 8.6 GPa with a volume collapse of 10.7%. The lattice

parameter in the B1 phase, which is 6.297 Å, underestimates the experimental value by 2.7%. The cell parameters in the PT structure are $a = 3.931$ Å, $c = 3.224$ Å which compares well with the experimental value [14].

Neither experimental nor theoretical information regarding the high-pressure structural behaviour are available for LaBi. In the present work a transition from B1 to PT is predicted around 11.2 GPa accompanied with a volume collapse of 7.83%. The value of lattice constant in B1 phase is 6.392 Å, which underestimates the experimental values by 2.6%. Similarly in PT structure the lattice parameters are $a = 4.023$ Å, and $c = 3.258$ Å. The bulk modulus in the B1 phase decreases as we go from LaSb to LaBi, and it is almost twice in the high-pressure PT phase.

3.2. Band structure and density of states

The self-consistent band structures for these compounds are obtained for both B1 and PT structures and are shown in Figs. 3 and 4. The overall band profile is found to be the same for both the compounds and is in good agreement with the earlier works [3,17]. From the band

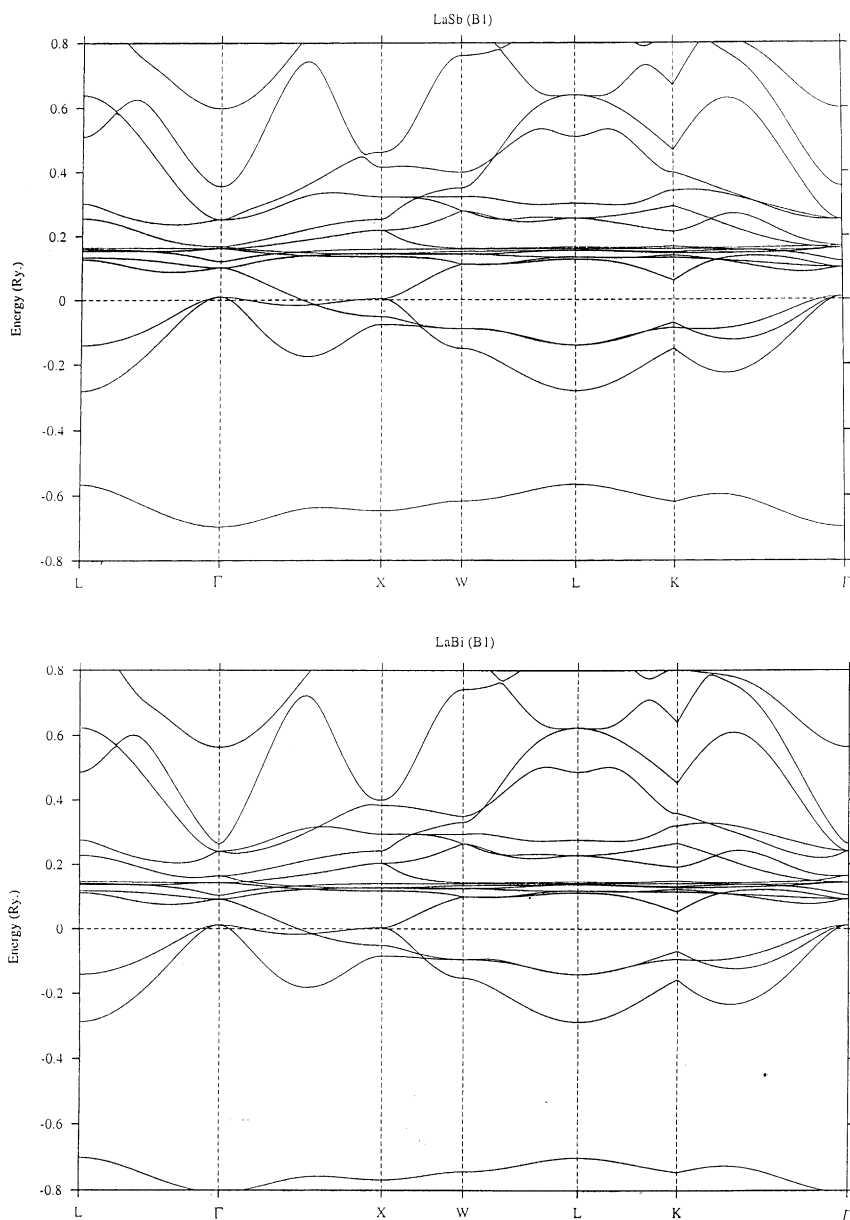


Fig. 3. Band structure in the B1 phase for (a) LaSb and (b) LaBi.

structure, it is seen that the lowest lying band in these compounds is mainly due to the pnictogen 's'-like state and it lies around -0.7 Ry in the case of LaSb. This band is slightly shifted in LaBi and lies around -0.82 Ry. The band lying above this is mainly due to the pnictogen 'p'-like states which

hybridizes with La 's'- and 'd'-like states at the Γ point. These hybridized bands lie slightly above the Fermi level when compared to other pnictides. This shift in these compounds may change the Fermi surface topology, which will lead to changes in the physical properties of these compounds. The

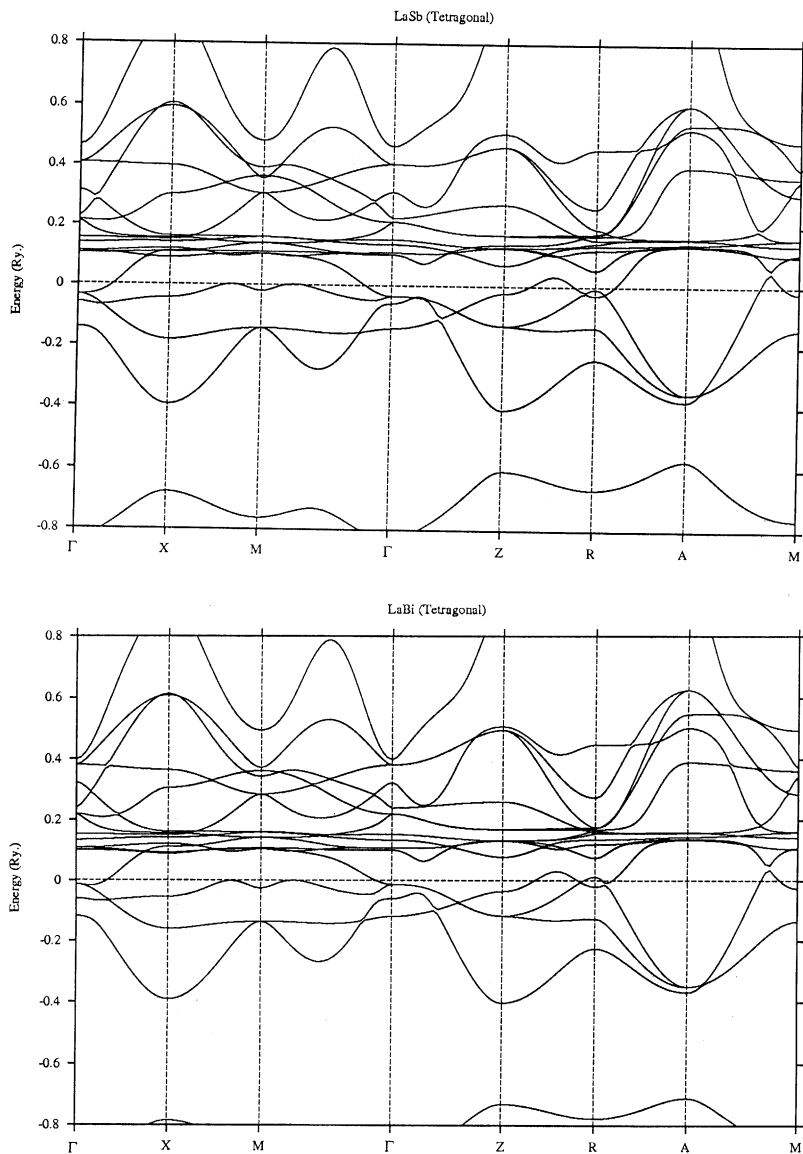


Fig. 4. Band structure in the PT phase for (a) LaSb and (b) LaBi.

narrow bands originating above the Fermi level are mainly due to La 'f'-like states. These bands are not completely localized and drop down below the Fermi level along the Γ -X direction. The major contribution to the density of states is mainly from La 'd'-like states which can be seen from the DOS histogram.

In the high-pressure phase of these compounds, there is an appreciable hybridization between La

'd'-like states and La 'f'-like states. Further the 'd'-like contribution at the Fermi level is more in the high-pressure when compared to the B1 phase. This may be one of the reasons for the increase in the density of states in the high-pressure PT phase.

The total and partial density of states of these pnictides is shown in Figs. 5 and 6. The DOS histogram of these pnictides in B1 phase consists of a peak present in the lowest energy part of the

DOS curve and is mainly due to the pnictogen ‘s’-like state. The region which lies above this is due to La ‘s’ followed by the contribution from La ‘d’-like and pnictogen ‘p’-like states which are degenerate up to the Fermi level. The regions, which lie above these states, are from La ‘f’-like states.

In the high-pressure phase, the contribution from the La ‘d’-like states is more at the Fermi

level compared with the La ‘f’ contribution. This ‘d’ contribution increases as one moves from LaSb to LaBi, which may be one of the reasons for the increase in the density of states in the high-pressure phase.

The electronic specific heat coefficient is calculated from the expression, $\gamma = \pi^2 k_B^2 N(E_F)/3$ using the calculated density of states at the Fermi energy. The calculated values are compared with

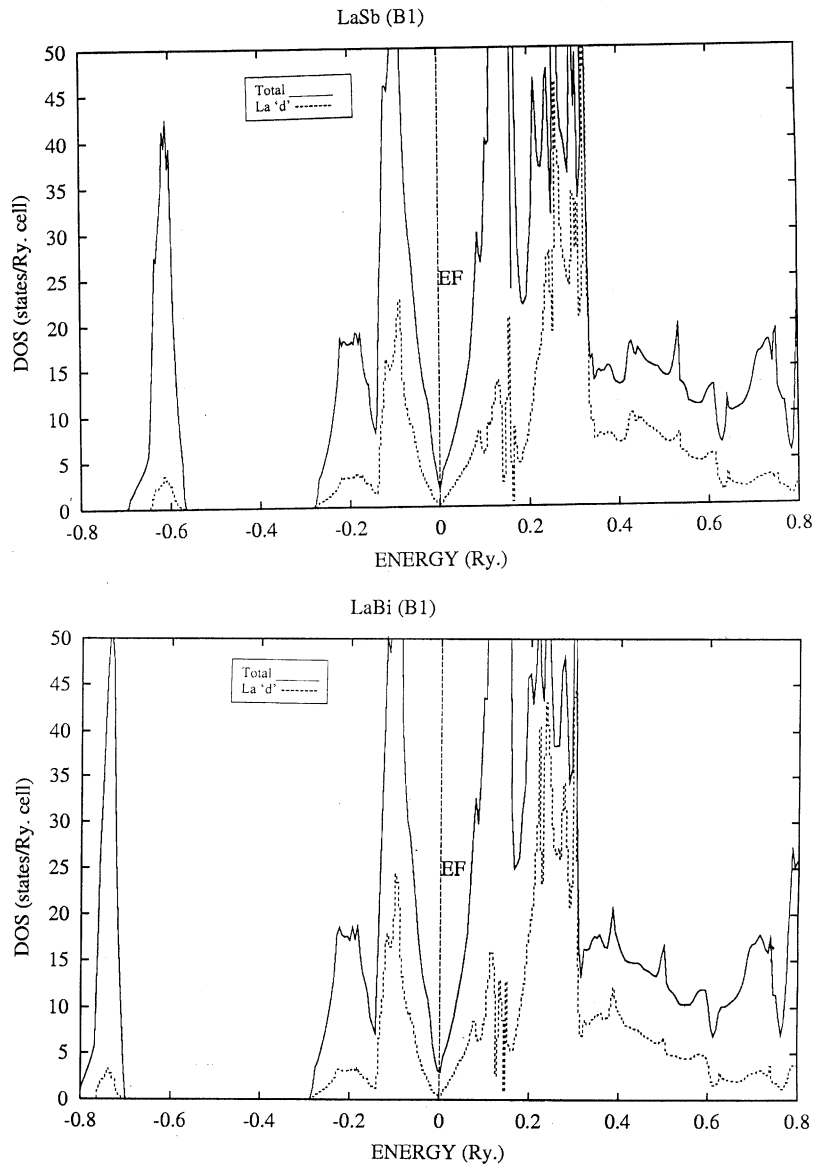


Fig. 5. Density of states in the B1 phase for (a) LaSb and (b) LaBi.

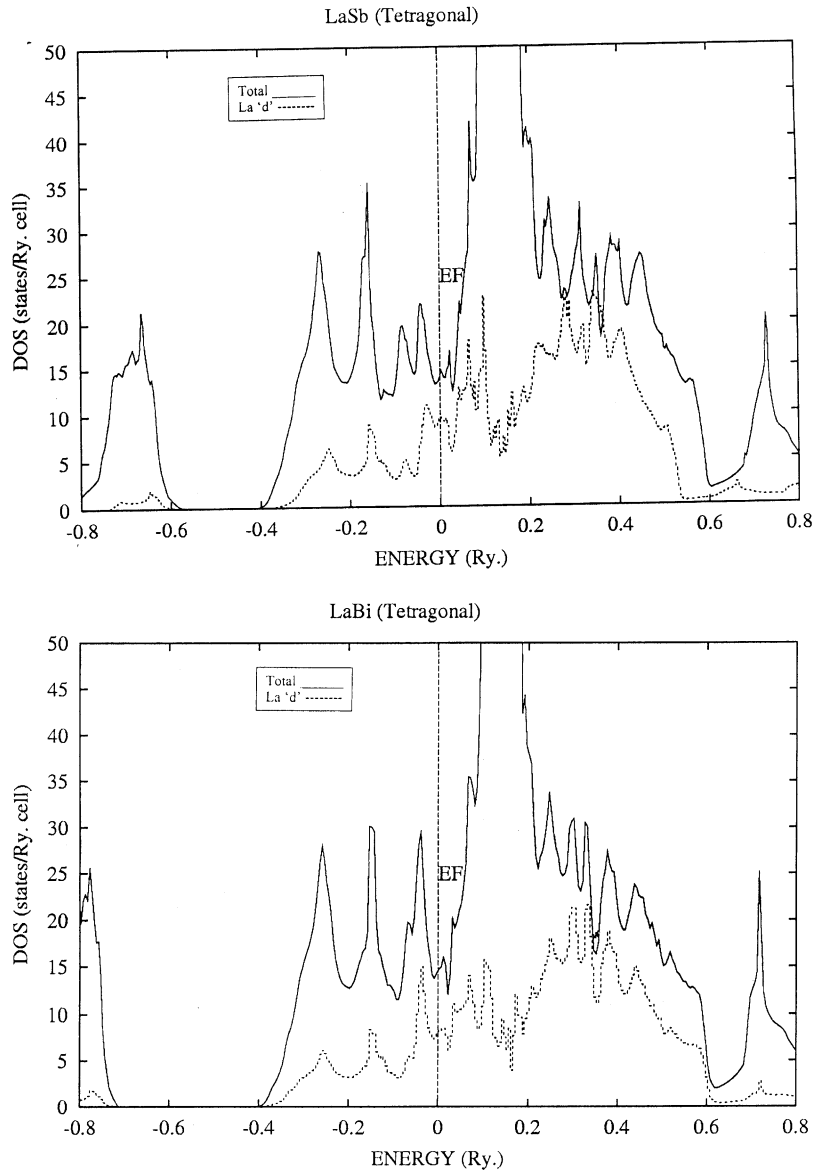


Fig. 6. Density of states in the PT phase for (a) LaSb and (b) LaBi.

the available experimental and theoretical values [17] and are tabulated in Tables 1 and 2.

The partial number of electrons is given in Table 4. From the table it is seen that there is a transfer of electrons from pnictogen 's' and 'p'-like states to the lanthanum 'd'-like states continuously under pressure, which may be responsible for the observed structural phase transformation.

4. Conclusions

Systematic tight binding linear muffin tin orbital calculations have been performed on LaSb and LaBi as a function of reduced volume. The present study confirms the experimental results that LaSb undergoes a structural phase transition from B1 to PT around 8.6 GPa and predicts that LaBi will

Table 4
Partial number of electrons as a function of V/V_0 for LaSb

V/V_0	Sphere radii (a.u.)		La				Sb	
	La	Sb	's'	'p'	'd'	'f'	's'	'p'
1.0	3.737	3.270	0.351	6.092	1.599	0.330	1.691	3.067
0.95	3.674	3.215	0.344	6.084	1.640	0.328	1.673	3.014
0.90	3.608	3.157	0.337	6.073	1.684	0.328	1.653	2.956
0.85	3.540	3.098	0.329	6.057	1.733	0.329	1.632	2.891
0.80	3.469	3.036	0.322	6.036	1.791	0.330	1.610	2.815
0.75	3.395	2.971	0.315	6.009	1.852	0.334	1.586	2.733
0.70	3.318	2.903	0.308	5.973	1.922	0.339	1.559	2.639

undergo a similar transition around 11.2 GPa. We hope that experiments can verify our prediction. Equilibrium lattice parameters and bulk moduli have been obtained and compared with available data. We find that the bulk moduli in the high-pressure phase are doubled when compared to ambient structure. This may be due to the increase in the covalent bond strength. The possible reason for the structural phase transition may be due to $sp \rightarrow d$ electron transfer under pressure.

References

- [1] F. Hulliger, Handbook on the Physics and Chemistry of Rare-Earths, in: K.A. Gschneidner, Jr., L. Eyring (Eds.), (Vol. 14), North-Holland, Amsterdam, 1979, p. 153 (Chapter 33).
- [2] H. Kitazawa, T. Suzuki, M. Sera, I. Oguro, A. Yanase, A. Hasegawa, T. Kasuya, J. Mag. Magn. 31–34 (1983) 421.
- [3] A. Hasegawa, J. Phys. Soc. Japan 54 (1985) 677.
- [4] Yasunori Kaneta, Osamu sakai, Tadao kasuya, Physica B 186–188 (1993) 156.
- [5] R. Settai, T. Goto, S. Sakatsume, Y.S. Kwon, T. Suzuki, T. Kasuya, Physica B 186–188 (1993) 176.
- [6] N. Mori, Y. Okayama, H. Takahashi, Y. Haga, T. Suzuki, Jpn. J. Appl. Phys. Suppl. 8 (1993) 182.
- [7] R. settai, T. Goto, S. Sakatsume, Y.S. Kwon, T. Suzuki, Y. Kaneta, O. Sakai, J. Phys. Soc. Japan 63 (1993) 3026.
- [8] M. Takashita, H. Aoki, T. Matumoto, C.J. Haworth, T. Terashima, A. Uesawa, T. Suzuki, Phys. Rev. Lett. 78 (1997) 1948.
- [9] J. Schoenes, B. Frick, O. Vogt, Phys. Rev. B 30 (1984) 6578.
- [10] H. Kumigashira, T.Ito Hyeong-Dokim, A. Ashihara, T. Takahashi, T. Suzuki, M. Nishimura, O. Sakai, Phys. Rev. B 58 (1998) 7675.
- [11] R. Settai, T. Goto, S. Sakatsume, Y.S. Kwon, T. Suzuki, T. Kasuya, Physica B 186–188 (1993) 176–178.
- [12] Y.S. Kwon, M. Takeshige, T. Suzuki, T. Kasuya, Physica B 163 (1990) 328.
- [13] T. Kasuya, Y. Haga, Y.S. Kwon, T. Suzuki, T. Suzuki, Physica B 186–188 (1993) 9.
- [14] J. Hayashi, I. Shihrotani, Y. Tanaka, T. Adachi, O. Shimomura, T. Kikegawa, Solid State Commun. 114 (2000) 561.
- [15] J.M. Leger, D. Ravot, J. Rossat-Mignod, J. Phys. C Solid state Phys. 17 (1984) 4935.
- [16] U. Benedict, J. Alloy Compounds 223 (1995) 216.
- [17] A. Hasegawa, J. Phys. C Solid State Phys. 13 (1980) 6147.
- [18] U. Benedict, S. Dabos-Seignon, J.P. Dancausse, M. Gensini, L. Gerward, R.G. Haire, J. Alloy Compounds 181 (1992) 1.
- [19] O.K. Andersen, Phys. Rev. B. 12 (1975) 3060.
- [20] H.L. Skriver, The LMTO Method, Springer, Heidelberg, 1984.
- [21] U. von Barth, L. Hedin, J. Phys. C. 5 (1972) 1629.
- [22] N.E. Christensen, D.L. Novikov, R.E. Alonso, C.O. Rodriguez, Phys. Stat. Sol. (b) 211 (1999) 5.
- [23] O.K. Andersen, J. Jepsen, Phys. Rev. Lett. 53 (1984) 2871.
- [24] O. Jepsen, O.K. Andersen, Solid State Commun. 9 (1971) 1763.
- [25] N.E. Christensen, Phys. Rev. B 32 (1985) 207.
- [26] A.G. Petukhov, W.R. Lambrecht, B. Segall, Phys. Rev. B. 53 (1996) 4324.
- [27] G. Kalpana, B. Palanivel, M. Rajagopalan, Phys. Rev. B. 50 (1994) 12318.
- [28] G. Kalpana, B. Palanivel, M. Rajagopalan, Phys. Rev. B. 52 (1995) 4.
- [29] F. Birch, J. Geophys. Rev. 83 (1978) 1257.
- [30] M. Born, K. Huang, Dynamical Theory of Crystal Lattices, Clarendon, Oxford, 1954.